DOI: 10.1002/chem.201500647

Helical Structures

Substituent Effects on the Photochromic Properties of Benzothiophene-Based Derivatives

Olivier Galangau,*[a, b] Takuyama Nakashima,[a] François Maurel,[c] and Tsuyoshi Kawai*[a, b]

Abstract: Five diarylethene photochromic derivatives, the structures of which incorporate a central benzothiophene unit, a left-hand thiazole group, and a right-hand benzothiophene group, have been prepared. The compound with a thiazole unit with no substituent on the reaction-center carbon atom reveals an unprecedented transformation upon light irradiation. When the 4-position of thiazole is protected by a methyl group, the compounds show high photosensitivity and photochromic properties. In this case, light irradiation affords new compounds with [5]helicene structures featuring the highest redshifted absorption maxima reported to date.

Introduction

Diarylethenes (DAEs) and their aromatic analogous derivatives have been the subject of intense research over the past two decades. These classes of compounds undergo reversible photoisomerization reactions between two stable forms: the ring-open form with the hexatriene backbone and the ring-closed form with the cyclohexadiene backbone.[1,2] Promising compounds centered on perfluorocyclopentene have shown high fatigue resistance and low thermal reactivity, which has made them highly attractive for optoelectronics applications.[3] However, their syntheses usually require the use of expensive and toxic octaperfluorocyclopentene, which inherently limits its use.[4] Consequently, a wide variety of heteroaromatic central bridging units have been introduced. Feringa et al. proposed to replace the perfluoro group with a perhydro group,[5a] whereas Hecht et al. suggested cyclopentene-related substances.[5b,6] Other groups have opted for aromatic rings, such as thiophenes,[7] *N*-methylindole,[8] indenones,[9] imidazoles,[10] thiazoles,[11] benzothiadiazoles,[12] or benzothiophene.[13] Recently, Guerchais et al. reported on CH direct arylation methodologies, involving benzothiophene as a central ring, which demonstrates how famous and attractive this heterocycle has become over the last few years.[14] Our group has also successfully employed this heterocyclic moiety as a centerpiece of a triangular (so-called terarylene) photoquantitatively ring-cyclized scaffold. Thanks to a series of intramolecular interactions that stabilize the photoreactive conformation, high photocyclization reactivity has been achieved.[13d] Herein, we wish to report on some related compounds based on the benzothiophene-centered terarylene backbone. We developed five derivatives with a pattern inspired by our previous results, comprising a left-hand thiazole group and a right-hand benzothiophene core. Minor changes in the substituents on the reaction centers were performed to investigate their influence on the overall photochromic properties. As shown herein, these slight perturbations in the molecular structure and on its symmetry have dramatic consequences for their photochromic features.

Results and Discussion

Syntheses

Details of the syntheses of precursor compounds are given in the Experimental Section. Compounds **3**, **4**, **5**, and **6** were prepared according to the synthetic route depicted in Scheme 1.

First, compounds **1a** and **1b** were converted into **2a** and **2b**, respectively, in very good yields, with Suzuki–Miyaura organometallic coupling conditions, as inspired by the work of Guglielmetti et al.[15b] Indeed, we found that the use of an activated palladium catalyst was necessary because the coupling involved two low-reactive positions (β–β coupling). From this perspective, DME has been known to enhance the reactivity of the palladium catalyst, probably due to strong chelation of the metallic center by the two oxygen atoms. The corresponding borylated reagents were prepared by conventional deprotonation with *n*BuLi and exchange with tributyl borate. These rela-

---

[a] Dr. O. Galangau, Dr. T. Nakashima, Prof. T. Kawai
International Collaborative Laboratory
Center for Frontier Science and Technology NAIST-CEMES
29, rue Jeanne Marvig, BP 94347, 31055 Toulouse (France)
E-mail: o-galangau@ms.naist.jp
tkawai@ms.naist.jp

[b] Dr. O. Galangau, Prof. T. Kawai
Graduate School of Materials Science
Nara Institute of Science and Technology, NAIST
8916-5 Takayama, Ikoma, Nara 630-0192 (Japan)
Fax: (+81) 743-72-6179

[c] Prof. F. Maurel
Laboratoire Interfaces, Traitements, Organisation et
Dynamique des Systèmes (ITODYS)
CNRS UMR 7086, Université Paris 7 - Paris Diderot
Sorbonne Paris Cité, Bâtiment Lavoisier
15 rue Jean Antoine de Bïf, 75205 Paris Cedex 13 (France)

Supporting information for this article is available on the WWW under http://dx.doi.org/10.1002/chem.201500647.

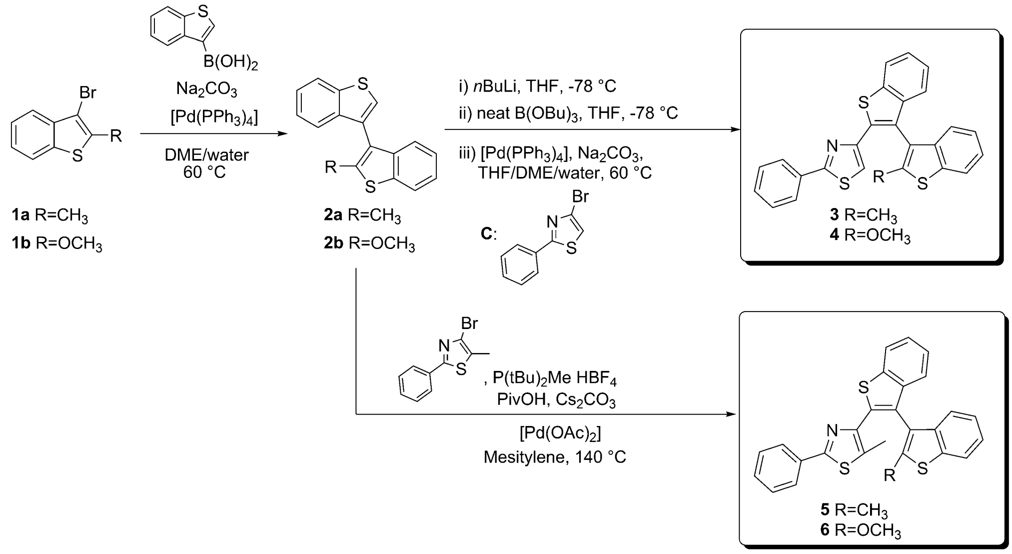

Scheme 1. Synthetic route to **2a**, **2b**, **3**, **4**, **5**, and **6**. DME = dimethoxyethane, PivOH = pivalic acid.

tively instable boronic esters were not isolated, but directly combined with precursor **C** to afford derivatives **3** and **4** in excellent yields. Derivatives **5** and **6** were obtained from the CH direct arylation coupling of intermediates **2a** and **2b** in good yields. The use of the standard Fagnou conditions (tricyclohexylphosphine combined with potassium carbonate in dimethylacetamide) did not give satisfactory results, which justifies the use of stronger conditions.[16] Finally, compound **9** was obtained from a different synthetic pathway (Scheme 2).

The CH direct arylation organometallic coupling with the strongest Fagnou conditions afforded intermediate **7** in excellent yield. A ratio of 3:1 thiazole/benzothiophene was necessary to maximize the reaction yield. Bromination of the β position on the benzothiophene core proceeded smoothly by using the combination of NBS in THF from low to room temperature, and **8** was employed without further purification. Eventually, modified Suzuki–Miyaura conditions afforded the target molecule **9** in excellent yield. Five sophisticated terarylene derivatives were prepared in high yields in a minimum of steps thanks to modular, efficient, and optimized synthetic approaches.

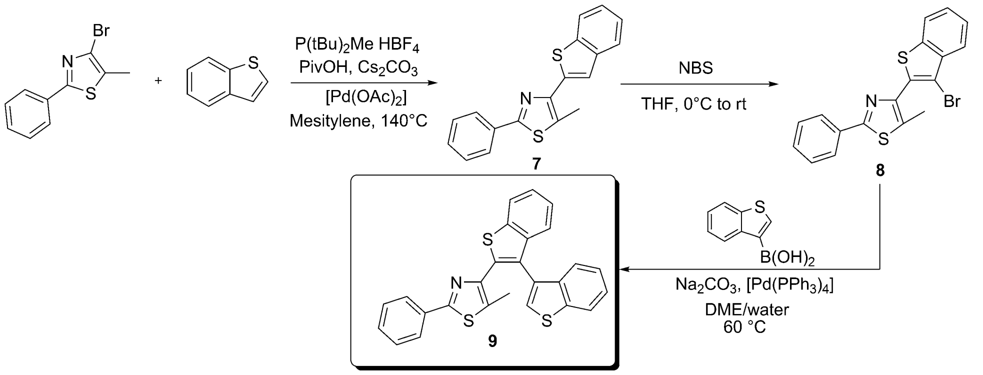

Scheme 2. Synthetic route to **7**, **8**, and **9**. NBS = *N*-bromosuccinimide.

Spectroscopic properties of derivatives 3 and 4

The spectroscopic properties of **3** and **4** were investigated in THF at room temperature and the results are gathered in Table 1. Both compounds showed similar characteristics, such as a maximum of absorption located in the UV wavelength range, at $\lambda = 314$ and 311 nm for **3** and **4**, respectively.

Upon UV-light irradiation, these compounds underwent a profound modification of their spectroscopic properties, as shown in Figure 1 by the emergence of new bands, especially in the visible part, with maxima located at $\lambda = 525$ nm for **3** and $\lambda = 543$ nm for **4**. These new absorption features can be safely assigned to the appearance of the corresponding closed-form isomers. However, these new bands thermally bleached a few seconds after irradiation stopped (dashed line in Figure 1), which indicated subsequent degradation of the closed-form adducts in both cases. These thermal bleaching reactions were studied in more detail by monitoring them with ^{1}H NMR spectroscopy and HRMS. After UV irradiation of the NMR spectroscopy tubes, the color faded quickly. The initial ^{1}H NMR spectrum of **3** showed quantitative conversion of the open isomer, as proven by the complete disappearance of the singlet at $\delta = 6.65$ ppm, which was assigned to the α-hydrogen atom on the thiazole ring, and the singlet at $\delta = 2.33$ ppm, which was assigned to the methyl group (see Fig-

Table 1. Spectroscopic properties of **3** and **4** in THF.

	λ_{max} [nm]	ε_{max} [L mol^{-1} cm^{-1}]	λ_{max} [nm]	ε_{max} [L mol^{-1} cm^{-1}]	$\Phi_{o/c}$[a]	$\Phi_{c/o}$
3 o	314	31 500	–	–	0.2 ± 0.1	–
3 c	–	–	525	–	–	–
4	311	28 500	–	–	0.3 ± 0.1	–
4 c	–	–	543	–	–	–

[a] Determined at $\lambda=313$ nm.

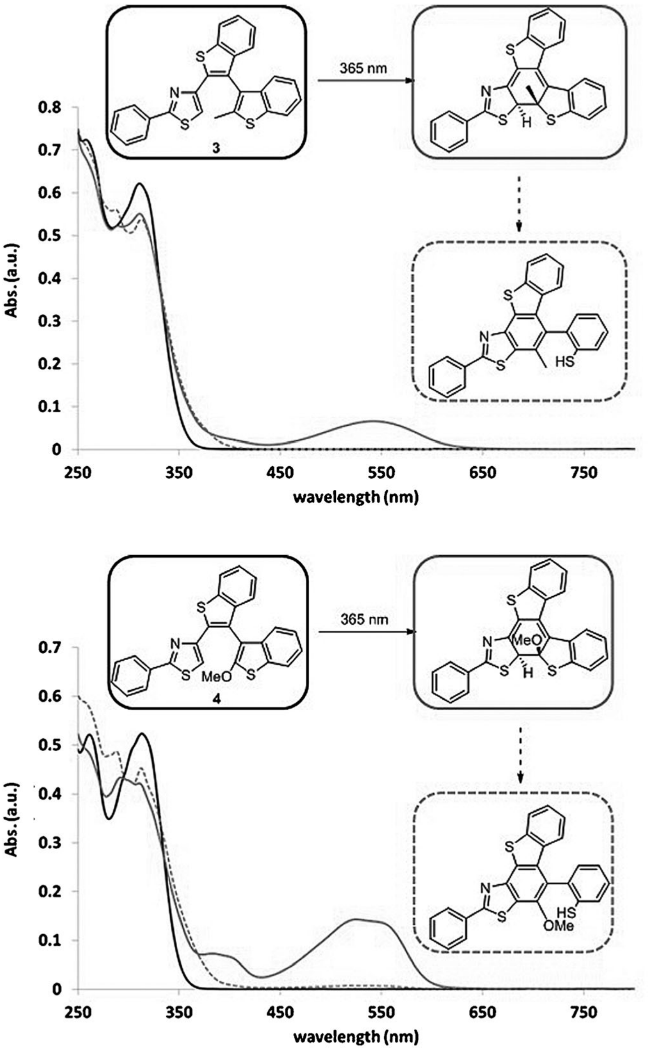

Figure 1. Absorption spectra of **3** (top) and **4** (bottom). Solid black line = open form, solid gray line = photostationary state, and dashed line = after thermal bleaching.

ure S3 in the Supporting Information). Instead, the two initial singlet signals were subjected to sizeable shifts: from $\delta=2.33$ to 2.42 ppm for the methyl signal and from $\delta=6.65$ to 3.81 ppm for the α-hydrogen atom. HRMS confirmed that the reaction proceeded without loss of atoms for both derivatives **3** and **4** (not shown).

The dark-state transformation also induces splitting in the aromatic area; the final spectrum displays nicely resolved signals (doublets, triplets). Krayushkin et al. recently reported dark bleaching processes that occurred in DAE-related substances possessing one hydrogen atom and a methyl group.[17] The 1D NOE and 2D experiments (COSY, HMQC, and HMBC) were carried out to determine the structure of the thermally generated byproduct (see Figures S5 and S6 in the Supporting Information). The HMQC experiment proved to be useful, since it showed that the singlet signal at $\delta=3.81$ ppm of one proton did not correlate with a carbon atom. The 1D NOE data also demonstrated a strong correlation between the methyl signal and the previous one (Figure 2), which meant that the two groups were close in space. Based on these considerations, we finally determined that, similarly to the report by Krayushkin et al.,[17] the closed-form adduct underwent a [1,5]-proton shift, followed by benzothiophene opening concomitant with the appearance of a fully aromatized derivative, which provided the driving force. Similar conclusions were drawn for compound **4** (see the Supporting Information). Assuming 1:1 photoreactions for **3** and **4**, we roughly evaluated their respective ring cyclization quantum yields to be 0.2 and 0.3 for **3** and **4**, respectively, in THF at room temperature. These values are also consistent with the population of the photoreactive conformer determined by variable-temperature (VT) NMR spectroscopy (see below) at the same temperature.

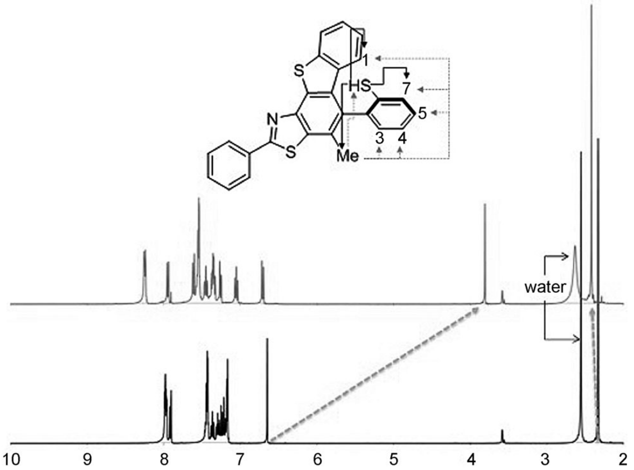

Figure 2. ^{1}H NMR spectra of **3** (lower spectrum = before irradiation, upper spectrum = after irradiation). Inset: Correlations observed by the 1D NOE experiment when the singlets at $\delta=3.81$ (solid line) and 2.42 ppm (dotted line) were irradiated.

Briefly, thanks to VT-NMR spectroscopy and quantum yield measurements, we clearly established that the photosensitivities of compounds **3** and **4** were rather low in THF at room temperature. They also displayed intriguing and unusual photochemical behavior because their corresponding closed-form isomers underwent rapid and quantitative bleaching, resulting in full aromatization of the core and benzothiophene ring cleavage.

Spectroscopic properties of derivatives 5, 6, and 9

Table 2. Spectroscopic properties of **5**, **6**, and **9** in THF.

	λ_{max} [nm]	ε (λ_{max}) [L mol^{-1} cm^{-1}]	λ_{max} [nm]	ε (λ_{max}) [L mol^{-1} cm^{-1}]	$\Phi_{o/c}$[a]	$\Phi_{c/o}$[b]	χ
5	304	22 200	540	13 000	0.73 ± 0.04	0.09	0.41
6	306	25 300	562	13 800	0.74 ± 0.04	$<$0.01	0.71
9[c]	305	25 400	544	–	–	–	–

[a] Absolute values determined at $\lambda = 313$ nm. [b] Absolute values determined at $\lambda = 540$ nm. [c] We were unable to evaluate the photoconversion, nor the quantum yields.

The properties of compounds **5**, **6** and **9** in THF were also investigated and the results are gathered in Table 2. These three compounds display very similar spectroscopic properties, as expected. Upon UV irradiation (Figure 3), their initial absorption spectra are deeply modified and new bands arise in the visible part at $\lambda = 540$ (**5**), 562 (**6**), and 544 nm (**9**). Notably, the OMe group of **6** induces a sizeable redshift (22 nm) of the closed-form absorption maximum compared with those of **5** or **9**, as well as band broadening. These photoprocesses seem to proceed in a clean way, as evidenced by the appearance of isobestic points at 322 (**5**), 310 (**6**), and 324 nm (**9**).

^{1}H NMR spectroscopic monitoring of their photoreactions also supports this observation and has allowed us to evaluate their respective photoconversion (see the Supporting Information). However, evaluating the photochromic parameters of compound **9** failed. None of the techniques (NMR spectroscopic monitoring or irradiation followed by HPLC separation) helped us to determine its photoconversion, probably because of secondary processes that hamper its evaluation. Therefore, only qualitatively spectroscopic results can be discussed for derivative **9**.

Their photoreversibility was also assessed by regenerating the open isomer under visible-light irradiation. The three derivatives showed poor fatigue resistances, even after one cycle, since the absorption spectra observed after visible irradiation did not match the initial ones (see the Supporting Information for more details). Such a result is in accordance with previous observations.[13b]

We also studied the thermal stability of the ring-closed forms, **5c**, **6c**, and **9c**. At high temperatures in toluene, all three derivatives underwent general bleaching accompanied by a monoexponential decrease in the absorbance. This suggests that temperature-dependent degradation occurs, and therefore, limits the stabilities of the closed forms. The Arrhenius plots of each of sample yielded the corresponding activation energies, along with the calculated half-lives at 298 K (see Table 3).

Compounds **5c** and **6c** feature similar activation energies of 100 and 105 kJ mol^{-1}, respectively, whereas **9c** shows the smallest activation energy (76 kJ mol^{-1}) along with the shortest half-life (about 24 days). This suggests that substituting the two reactive carbon sites enhances the stability of the thermal closed-form adduct. Notably, upon going from **3c** and **4c** to **9c**, that is, when switching the position of the hydrogen atom from one ring to another, significant improvement of the stability of the closed isomer was achieved from few minutes to several days.

Ultimately, we evaluated the photochromic efficiencies of these three derivatives by measuring their ring cyclization and ring cycloreversion quantum yields in THF at room temperature. For both **5** and **6**, we measured large improvements of $\Phi_{o/c}$ compared with those of **3** and **4**, respectively.

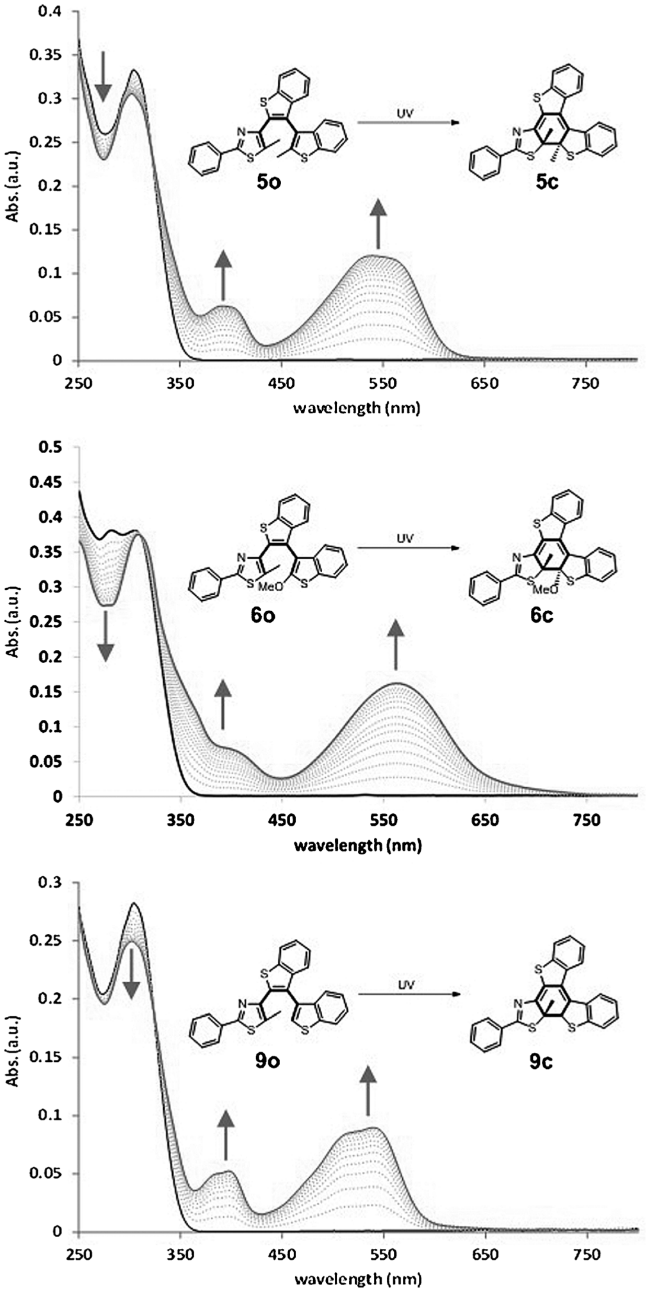

Figure 3. UV/Visible spectra of **5** (top), **6** (middle), and **9** (bottom). Solid black line = open isomers. Solid gray line = Photo-stationary state.

Table 3. Calculated activation energies for the thermal degradation of derivatives **5c**, **6c**, and **9c**.

	E_a [kJ mol^{-1}]	$t_{1/2}$ [days] at 298 K
5c	100	103
6c	105	144
9c	76	24

Table 5. Computed conformational exchange of **3a** and **3b** at 298 K.

	Conformer	d_{NS} [Å]	T_1 [°]	T_2 [°]	Population AP [%]	Population P [%]	ΔE [kcal mol^{-1}]
3	AP	2.93	−16	111	44	–	0.14
	P	2.94	11	69	–	56	
4	AP	3.02	−25	111	36	–	0.33
	P	2.93	6	70	–	64	

Indeed, compounds **5** and **6** feature high values of around 70 %, which makes them very photosensitive. These results demonstrate 1) that substitution on the benzothiophene unit has a small influence on the photosensitivity (no change between **5** and **6**), and 2) the substitution of the reactive site on the thiazole group plays a major role in stabilizing the photoreactive conformer in solution (e.g., **3** vs. **5**). We suggest herein the existence of weak intramolecular interactions, such as CH–π bonding interactions, occurring between the methyl group attached to thiazole and benzothiophene. Such an interaction would partly drive the conformational equilibrium toward the antiparallel (AP) conformer. Quantum yields and VT-NMR spectroscopy (see below) measurements suggest that the ring cyclizations reflect, at least partly, the solution equilibrium state. For $\Phi_{c/o}$, the trend is reversed. Introducing a methoxy group onto the molecular backbone quenches cycloreversion; this is known for other DAEs.[18]

VT-NMR spectroscopy data

NMR spectroscopy measurements have already proven to be a valuable tool to examine the equilibrium between parallel (P) and antiparallel (AP) conformers in solution that limits the ring cyclization efficiency.[19] To determine whether the photocyclization reactivity was limited by such an equilibrium, we monitored specific chemical shifts in [D$_8$]THF (see the Supporting Information) as a function of the temperature (from 193 to 333 K). No splitting of signals was observed, which meant an equilibrium was rapidly set up at each temperature. Results are summarized in Table 4. Assuming fast equilibrium between the two conformers (AP and P), we could calculate their respective Boltzmann populations at 298 K (Table 5).

Thus we obtained clear evidence that, if the methyl group is positioned on the thiazole or benzothiophene moieties, the population ratio is reversed. Although **3** and **4** show weak photosensitivity (less than 30 %), compounds **5**, **6**, and **9** display high photosensitivity, with population of the photoreactive conformer of 70 %. This fact strongly suggests that, since the molecule is nonsymmetric, benzothiophene and thiazole must play different roles in the conformation equilibrium (**3** vs. **9**). We propose herein that a CH–π interaction is established between benzothiophene (π group) and the methyl group attached to thiazole. This attractive interaction is then likely to stabilize the AP conformation, and therefore, drives the equilibrium. Notably, these data match the previously mentioned quantum yields well, and therefore, clearly demonstrate that, for the whole compound family, the photocylizations are limited by their conformational exchange only, and the reactive conformers undergo photon-quantitative cyclization.

Table 4. Calculated populations of the conformers and free Gibbs energy at 298 K.

	Population of conformers AP [%]	Population of conformers P [%]	ΔG^0 [kcal mol^{-1}]
3	24	76	−0.7
4	28	72	−0.6
5	68	32	0.5
6	71	29	0.6
9	69	31	0.5

To summarize, as opposed to previous results, thanks to VT-NMR spectroscopy and photochemical measurements in THF, we have demonstrated that adding a methyl group to the thiazole unit dramatically improves both the photosensitivity and chemical stability in the dark for the closed-form adduct. However, when the two reactive carbon atoms are substituted by groups other than hydrogen atoms, the stability is improved. Moreover, it is worth mentioning that small variations of ΔG^0 achieved by removing one methyl group induce remarkable large discrepancies in the population ratio of reactive/nonreactive isomers, which underlines the difficulty of rationally designing highly photosensitive DAE systems.

Theoretical investigations

Computations were performed on the five derivatives to gain a better insight into their conformational, electronic, and UV/Visible properties. We performed calculations by using the Gaussian 09 (see the Supporting Information for a full reference) package by using a combination of the ωB97XD functional and the 6-31G(d) basis set for geometrical optimizations (ωB97XD/6-31G(d) calculations). Conformational analyses were performed on the open isomer of compounds **3** and **5**. TD-DFT calculations were carried out at the ωB97XD/6-311g(d,p) level of theory. NMR spectroscopy predictions were performed at the PBE0/6-311++g (2d,p) level. In the case of the non-photoreactive conformers, geometries corresponding to an energy minimum were reoptimized at the same level of theory prior to NMR spectroscopy calculations. Conformational equilibria of compounds **4**, **6**, and **9** were studied by considering the relevant geometries established with scans performed on **3** and **5**. IR spectra of the optimized structures showed no imaginary frequencies, which suggested that they corresponded to energy minima. TD-DFT calculations of open-form isomers were achieved based on the geometries of photoreactive conformers.

Geometrical considerations on 3 and 4

Geometrical optimizations were performed for each of the compounds in vacuo (see the Supporting Information). In the case of **3** and **4**, the lowest energetic geometry corresponds to a non-photoreactive one (see Figure 4).

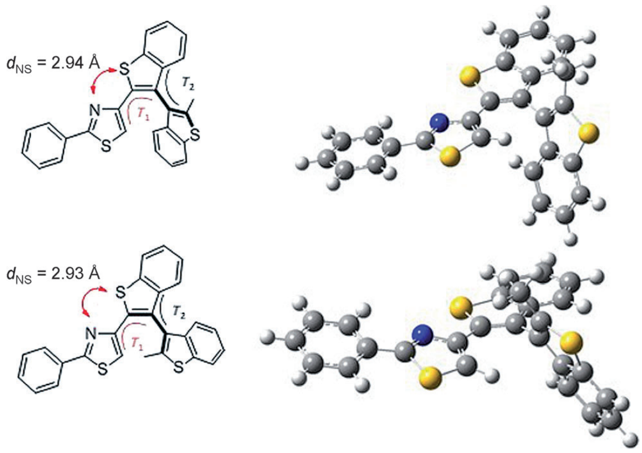

Figure 4. Predicted geometries of **3** for the lowest (top) and highest (bottom) energy configurations.

Computations predicted almost coplanarity between the thiazole and central benzothiophene groups, with a nitrogen–sulfur distance (d_{NS}) of 2.94 Å for both compounds; this is in the range of attractive N–S bonding interactions.[13d,20] In the case of **3**, the two torsion angles, T_1 and T_2, were calculated to be 11 and 69°, respectively. The former value indicates again the coplanarity of both thiazole and benzothiophene. The latter suggests that the end of benzothiophene must be disconnected from the rest of the molecule, probably because of strong steric repulsions. From this perspective, it is clear that the substituent at the end of benzothiophene has a minor role to play into the relative stability of the geometry, since it is projected outwards. In addition, computations allow us to reproduce the conformational equilibrium by scanning the T_2 value and fully optimizing the resulting geometry at each step. Starting from the lowest energy geometry and rotating the benzothiophene group counterclockwise, calculations predict a second energy minimum, lying at slightly higher energy ($\Delta E = 0.14\ \mathrm{kcal\,mol^{-1}}$), corresponding to an AP conformation. This conformer shows torsion angles of $T_1 = -16°$ and $T_2 = 111°$, along with a P/AP ratio of 56%/44%. Although calculations significantly overestimate these population ratios, one should consider that computations reproduce the conformational equilibrium well. Similar conclusions can be drawn for compound **4**, for which the calculations predict a slightly improved AP population (36%) with an energy gap of 0.33 kcal mol^{-1}.

Geometrical considerations on open isomers 5, 6, and 9

We proceeded in a similar way to compute the geometries of **5o**, **6o**, and **9o** (Figure 5). For the three derivatives, the lowest energetic configuration corresponds to an AP conformation within both thiazole and benzothiophene groups to form large torsion angles ($T_1 = -47°$, $T_2 = 121°$).

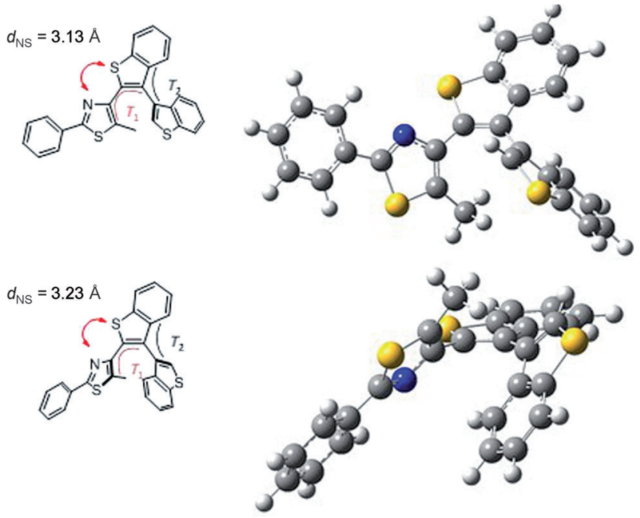

Figure 5. Predicted geometries of **9o** for the lowest (top) and highest (bottom) energy configurations.

Similar to **3**, computation of the equilibrium was also performed on compound **5o** (see Figure S16 in the Supporting Information). Three P conformations, P_1, P_2, and P_3, were found. The last two lie at high energies (2.24 kcal mol^{-1} for P_2 and 2.98 kcal mol^{-1} for P_3, as referenced to the lowest energy geometry), whereas P_1 is only about 0.65 kcal mol^{-1} higher than the energy minimum. Therefore, conformations P_2 and P_3 should be barely populated at room temperature. Calculated Boltzmann populations based on the computed energy gap separating the AP and P conformers affords a 72%/28% ratio for **9o**, which is consistent with experimental VT-NMR spectroscopy observations (Table 6). Similar conclusions can be drawn for compounds **5o** and **6o**. As observed by a comparison between **5o**, **6o**, and **9o**, the substituent located on the benzothiophene has a limited impact on the equilibrium, as expected and observed in solution. However, going from **3** to **9** clearly demonstrates the key role of the substituent located on thiazole. Thus, we calculated the distance between the methyl positioned on the thiazole and benzothiophene planes, in their respective AP conformations (Table 6). The three derivatives are predicted to show rather short distances of about 2.8 Å, corresponding to typical distances involving CH–π bonding interactions. However, since we were unable to provide experimental data for comparison, we suggest the existence of interactions (attractive or repulsive) that force the molecular scaffold to adopt the AP conformation.

As a result, DFT calculations are in reasonable agreement with the experimental observations. The existence of confor-

Table 6. Computed conformational exchange of **5**, **6** and **9** at 298 K.

	Conformer	d_{NS} [Å]	T_1 [°]	T_2 [°]	Population AP [%]	Population P [%]	ΔE [kcal mol^{-1}]	$d_{CH-\pi}$ [Å]
5o	AP	3.15	−49	12	75	–	0.65	2.75
	P	3.23	53	62	–	25		–
6o	AP	3.22	−53	122	79	–	0.77	2.81
	P	3.21	50	58	–	21		–
9o	AP	3.13	−47	121	72	–	0.56	2.75
	P	3.23	52	54	–	28		–

mational equilibria is predicted and the influence of substitution on the most stable molecular geometry is also demonstrated; this is consistent with the VT-NMR data.

Recently, Yang et al. developed a new methodology to reveal the existence of weak noncovalent interactions (NCIs).[21] When comparing the three photoreactive conformers, a persistent attractive NCI (green surfaces in Figure 6) occurred between the adjacent benzothiophene group and methyl attached to the thiazole group, which was in agreement with our previous DFT findings. Surprisingly, a second attractive interaction between the two benzothiophene moieties (Figure 6 and Figure S17 in the Supporting Information) contributes to stabilization of the conformation. Moreover, additional interactions are foreseen between the substituent on benzothiophene and the thiazole group for compounds **5o** and **6o** (see Figure S17 in the Supporting Information). These theoretical observations tend to validate the concept of weak interactions, such as CH–π attractive interactions, that also stabilize the photoreactive conformer.

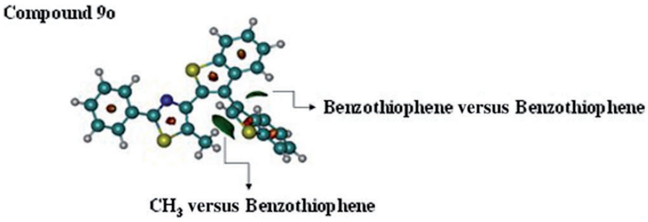

Figure 6. Visualization of the weak attractive NCIs in compound **9o**.

Calculated NMR spectroscopy considerations on 5, 6, and 9 open isomers

To further prove the correlation between calculations and experimental data, we computed the NMR spectra of both conformers for each of the samples **5o**, **6o**, and **9o** (see the Supporting Information for the methodology). The theoretical chemical shift assigned to the methyl substituent located on the thiazole ring was then calculated in vacuo at the PBE0/6-311g(2d,p) level of theory.[19c]

As observed from the results in Table 7, calculations predict slightly overestimated values for AP conformers, whereas the chemical shifts of the P conformers are underestimated. However, the general trend observed from VT-NMR spectroscopy data is well reproduced by DFT calculations.

These overall outcomes tend to demonstrate that DFT calculations fairly reproduce the experimental observations with quite large discrepancies, depending on the molecules under study.

Table 7. Agreement of the NMR spectroscopy computations with the VT-NMR data.

	Conformer	δ_{VT} [ppm]	δ_{DFT} [ppm]	R [%][a]
5o	AP	1.42	1.67	17
	P	2.58	1.99	−23
6o	AP	1.76	1.79	2
	P	2.64	2.05	−22
9o	AP	1.42	1.57	10
	P	2.56	1.73	−32

[a] $R=[(\delta_{DFT}-\delta_{VT})]/\delta_{VT}\times 100$, in which δ_{DFT} and δ_{VT} are the chemical shifts determined by DFT calculations and VT-NMR spectroscopy, respectively.

While the computed properties of compounds **3** and **4** poorly match the experimental results, those of derivatives **5o**, **6o**, and **9o** are, on the contrary, well reproduced. For **5o**, **6o**, and **9o**, computations show a clear combination of weak noncovalent nitrogen–sulfur interactions, steric repulsion, and weak methyl/benzothiophene interactions that eventually result in stabilization of the AP conformation. DFT calculations found reasonably good agreement for the conformational equilibrium and predicted NMR spectra.

Geometrical considerations on closed isomers 5, 6, and 9 (5c, 6c, and 9c)

We also investigated the corresponding closed forms of **5**, **6**, and **9** from the structural point of view (Figure 7).

In the closed form, the reactive carbon sites change their hybridization from sp^2 to sp^3, as predicted by their adopted tetrahedral shape. Interestingly, the nitrogen and sulfur centers are found at a distance of 3.15 Å for all derivatives, which means that the two still interact. Additionally, optimized structures

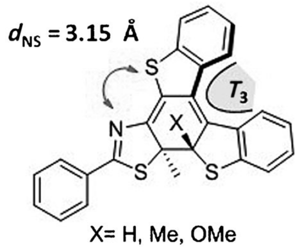

Figure 7. Predicted geometries for **5c**, **6c**, and **9c**.

show clear characteristics of the helical backbone, with five fused ring members connected to each other.[22] As a result, a twist angle, T_3, of 41° is formed between the two terminal moieties. Although [5]helicenes or related substances are rare, mainly due to their difficult preparation methods,[23] similar values of helical curvature have been reported.[22b]

TD-DFT investigations into open isomers of 3, 4, 5, 6, and 9

To gain a better insight into the photochemical properties of the compounds, we performed TD-DFT calculations in vacuo. We present hereafter calculated vertical transitions of the five open isomers of **3**, **4**, **5**, **6**, and **9** (see also the Supporting Information). All open forms of the compounds display rather usual photochromic properties. TD-DFT calculations predict maxima of absorption located in the UV part of the electromagnetic spectra with a constant error relative to the experimental data (see Table 8).

Table 8. Agreement of the vertical transitions with the UV/Visible data.

	λ_{exptl} [nm]	λ_{TD} [nm]	$\Delta\lambda$ [nm]
3	311	283	28
4	314	281/279	33/35
5 o	304	277	27
6 o	305	280	25
9 o	306	278	28

The HOMOs exhibit conventional antibonding interactions between the two carbon sites, whereas those of HOMO-1 show opposite bonding interactions. As usually observed for DAE and terarylene derivatives, the first transition is characterized by a small oscillating strength value, which is correlated herein with the fact that the density flows from the two benzothiophenes to the thiazole unit, resulting in poor overlap between the two series of molecular orbitals (charge-transfer excitation). Surprisingly, the photochromic virtual molecular orbital, that is, the one populated after electronic excitation and triggering the bond-forming step, does not correspond to the LUMO, but to the LUMO+1. Indeed, as seen in the Supporting Information, for all derivatives, the LUMO+1 presents an adequate bonding interaction, whereas the LUMO shows the absence of density on one of the reactive carbon sites. Therefore, the photochromically active transitions, herein $S_0 \rightarrow S_2$, are mainly dominated by a density flow of HOMO→LUMO+1.

TD-DFT investigations into closed isomers of 5, 6, and 9 (5 c, 6 c, and 9 c)

Vertical transitions of derivatives **5 c**, **6 c**, and **9 c** were computed at the same level of theory. All show identical photophysical behavior (Table 9), with theoretical absorption spectra matching those obtained experimentally within reasonable error values.

Note that the calculations reproduce well the redshift of the absorption maximum in **6 c** relative to the rest of the family.

Table 9. Agreement of the vertical transitions with the UV/Visible data.

	λ_{exptl} [nm]	λ_{TD} [nm]	$\Delta\lambda$ [nm]
5 c	540	560	18
6 c	562	571	24
9 c	544	537	21

The visible band was assigned to a pure HOMO→LUMO transition in charge of the photochromic reaction. Indeed, although the HOMOs present a typical bonding interaction, the LUMOs display a characteristic antibonding one. Our molecular systems compete well with previously published derivatives.[22b,e–f] Absorption maxima are all redshifted by about 40 to 60 nm, with a large increase in the molecular extinction coefficient values, although their photoconversions are fairly similar to those reported by the Yokoyama group.[22b]

Conclusion

We prepared five photoactive compounds based on the terarylene model, incorporating a central benzothiophene moiety, a left-hand thiazole group, and a right-hand benzothiophene one. Two categories of derivatives could be suggested, depending on whether the thiazole was substituted or not. When it was unsubstituted, these derivatives featured complete phototransformations into new aromatic derivatives functionalized by a thiol group.

On the other hand, effective photochromic behavior was observed in compounds with a thiazole unit substituted by a methyl group. In other words, ring cyclization was characterized by high quantum yield values, moderate to high photoconversions, and afforded stable helical closed isomers, which were the first of their kind to absorb far in the visible range.

On the basis of VT-NMR spectroscopy experiments and ring cyclization quantum yield measurements in solution, we clearly established that the photosensitivity of the open isomers was strictly limited by their ground-state conformational exchange. Theoretical computations afforded an understanding of the conformational equilibrium by mimicking the experimental data. They clearly revealed additional weak intramolecular interactions to stabilize the AP conformer for **5**, **6**, and **9**. On the contrary, in scaffolds **3** and **4**, such interactions vanished and the photosensitivities were therefore lower. We are now focusing our efforts on the enantioselective photogeneration of similar helical closed isomer and, in the meantime, trying to improve their overall stability.

Experimental Section

Chemicals/purification/analyses

Chemicals were purchased from Tokyo Chemical Industries, Wako Chemicals, and Sigma Aldrich and were used without any further treatment. Dry solvents were purchased from Nacalai Tesque and Sigma Aldrich, and kept under a nitrogen atmosphere. Spectroscopic-grade solvents were purchased from Wako chemicals. ^{1}H and ^{13}C NMR spectra were recorded on a JEOL JNM-AL-300 (300 MHz) and JEOL JNM-ECP400 (400 MHz) spectrometers. The 2D NMR spectra were recorded on a JEOL ECA-600 MHz spectrometer. Chemical shifts were referenced to the residual solvent signals. Mass spectra were measured with a JML-700 (EI) mass spectrometer. ATR-IR spectra were recorded on a JASCO FT/IR-4200 spectrometer with an ATR PRO410-S attachment. Melting points were measured with a capillary MEL-TEMP apparatus. Purifications by flash chromatography were performed on a YAMAZEN W-Prep 2XY system. Compounds studied by spectroscopic measurements of any kind were first purified by either HPLC (normal phase: HITACHI, LaChrom ELITE, L-2400 as detector,L-2130 as pump, D-2500 as integrator with a Nacalai Tesque, COSMOSIL 55 L-II, 20×250 mm packed column and reversed phase: LaChrom ELITE, L-2455 as detector, L-2130 as pump with a Nacalai Tesque COSMOSIL 5C$_{18}$ 201D×250 mm packed column) or GPC (8391 NEXT HPLC from Japan Analysis Industry).

Photophysical studies

Absorption spectra were recorded with spectrophotometers (JASCO V-670 and V-660). A Compact Asahi spectra xenon light source was used as an irradiation source. Light with an appropriate wavelength was obtained by being passed through additional filters. Absolute ring cyclization quantum yield values were obtained on a Shimadzu QYM-01 setup. Ring cyclization reaction quantum yields of instable derivatives were measured relative to the reference compound 1,2-bis(2-methylbenzo[*b*]thiophene-3-yl)perhexafluorocyclopentene, the value of which was 0.35 under $\lambda = 313$ nm light irradiation in hexane (see the Supporting Information for a reference), by determining their respective photoconversion under identical irradiation conditions. The relative quantum yields were obtained from the relationship expressed in the Supporting Information.

Synthesis of 2a

A Schlenk tube equipped with a magnetic stirring bar and capped with a rubber septum was charged with **1a** (1.28 g, 5.6 mmol, 1 equiv), commercially available benzo[*b*]thiophen-3-ylboronic acid (1.5 g, 8.4 mmol, 1.5 equiv), and anhydrous sodium carbonate (0.893 g, 8.4 mmol, 1.5 equiv). DME (169 mL) was then added and the suspension was evacuated/backfilled with nitrogen several times. Tetrakis(triphenylphosphine) palladium(0) (0.195 g, 3 mol%) was added under a stream of nitrogen followed by distilled water (84 mL), and the monophasic mixture was evacuated/backfilled again. The solution was heated at 75–85 °C over a period of 24 h (TLC monitoring) and was allowed to cool to RT. After diluting the mixture with water, the aqueous layer (purple) was extracted with ethyl acetate several times. The organic phases were combined, dried over anhydrous magnesium sulfate, filtered, and the solvent was removed. The crude product was purified by column chromatography (silica, hexane) to give **2a** as a white solid (1.41 g, 90%). M.p. 65–70 °C; ^{1}H NMR (300 MHz, CDCl$_3$): $\delta = 2.44$ (s, 3H), 7.22–7.44 (m, 6H), 7.54 (s, 1H), 7.81 (d, 1H, $J = 6$ Hz), 7.95 ppm (d, 1H, $J = 6$ Hz); ^{13}C NMR (75 MHz, CDCl$_3$): $\delta = 14.8$, 122.0, 122.6, 122.8, 123.2, 123.4, 123.9, 124.1, 124.2, 124.3, 124.5, 124.6, 124.7, 125.6, 127.5, 130.7, 138.2, 138.3, 138.8, 140.0, 140.4 ppm; IR: $\tilde{\nu} = 3086$, 3056, 1452, 1422, 1344, 1314, 1253, 1180, 1153, 1019, 797, 757, 727 cm^{-1}; HRMS (EI): *m/z* calcd for $C_{17}H_{12}S_2$ [M^+]: 280.0380; found: 280.0372.

Synthesis of 2b

A Schlenk tube equipped with a magnetic stirring bar and capped with a rubber septum was charged with compound **1b** (1.37 g, 5.6 mmol, 1 equiv), commercially available benzo[b]thiophen-3-ylboronic acid (1.5 g, 8.4 mmol, 1.5 equiv), and anhydrous sodium carbonate (0.893 g, 8.4 mmol, 1.5 equiv). DME (140 mL) was then added and the suspension was evacuated/backfilled with nitrogen several times. Tetrakis(triphenylphosphine) palladium(0) (0.195 g, 3 mol%) was added under a stream of nitrogen followed by distilled water (70 mL), and the monophasic mixture was evacuated/backfilled again. The solution was heated at 75–85 °C over a period of 24 h (TLC monitoring) and allowed to cool to RT. After diluting the mixture with water, the aqueous layer (purple) was extracted with ethyl acetate several times. The organic phases were combined, dried over anhydrous magnesium sulfate, filtered, and the solvent was removed. The crude product was purified by column chromatography (silica, hexane to mixture hexane/CHCl$_3$, 9/1, v/v) to give 2b as a white solid (1.3 g, 78%). M.p. 147–149 °C; ^{1}H NMR (300 MHz, CDCl$_3$): $\delta = 3.93$ (s, 3H), 7.22–7.39 (m, 5H), 7.49 (s, 1H), 7.57 (d, 1H, $J = 6$ Hz), 7.71–7.74 (m, 2H), 7.92 ppm (d, 1H, $J = 6$ Hz); ^{13}C NMR (75 MHz, CDCl$_3$): $\delta = 61.6$, 109.74, 121.8, 122.2, 122.7, 122.9, 123.6, 123.9, 124.3, 124.7. 125.5, 125.6, 128.7, 130.9, 138.4, 138.5, 139.9, 161.1 ppm; IR: $\tilde{\nu} = 3090$, 3051, 2922, 2851, 2831, 1594, 1577, 1544, 1498, 1456, 1420, 1319, 1266, 1256, 1224, 1152, 1070, 1011, 766, 749, 726 cm^{-1}; HRMS (EI): *m/z* calcd for $C_{17}H_{12}OS_2$ [M^+]: 296.0330; found: 296.0330.

Synthesis of 3

A flame-dried Schlenk tube was charged with **2a** (500 mg, 1.8 mmol, 1.5 equiv) and dry THF (approximately 30 mL). The solution was cooled to −78 °C before a solution of *n*BuLi in hexane (1.6 м, 1.79 mL, 1.6 equiv) was added dropwise by means of a syringe. The solution turned brown and after 45 min at that temperature neat tributylborate (0.481 mL, 1.8 mmol, 1.5 equiv) was added. The low-temperature bath was removed and the solution was allowed to warm to RT over a period of 1 h or more. In the meantime, the solution turned red and then pale orange. Finally, the content was transferred by means of a syringe to a second Schlenk tube containing 4-bromothiazole (286 mg, 1.2 mmol, 1 equiv), sodium carbonate (189 mg, 1.8 mmol, 1.5 equiv), and tetrakis(triphenylphosphine) palladium(0) (41 mg, 3 mol%) dissolved into a degassed 1:1 mixture of DME/water mixture. The combined solution was warmed at 65–75 °C until TLC showed reaction completion. The crude product was allowed to cool to RT, diluted with water, and extracted with ethyl acetate. The organic phases were combined, dried over anhydrous magnesium sulfate, filtered, and the solvent was removed. Purification by flash chromatography (silica, hexane/CHCl$_3$, 9:1, v/v) afforded **3** as a white powder (470 mg, 90%). M.p. 70–75 °C; ^{1}H NMR (300 MHz, CDCl$_3$): $\delta = 2.33$ (s, 3H), 6.53 (s, 1H), 7.19–7.46 (m, 9H), 7.87–7.98 ppm (m, 4H); ^{13}C NMR (75 MHz, CDCl$_3$): $\delta = 14.5$, 114.3, 119.2, 122.2, 122.3, 122.4, 122.7, 123.2, 124.2, 124.4, 124.5, 124.6, 124.9, 126.0, 126.6, 127.4, 128.9, 130.2, 133.1, 138.7, 139.0, 139.1, 139.3, 140.8, 149.4, 166.8 ppm; IR: $\tilde{\nu} = 3116$, 3054, 2847, 1505, 1482, 1456, 1437, 1312, 1250, 1172, 1152, 1014, 965, 782, 759, 733 cm^{-1}; HRMS (EI): *m/z* calcd for $C_{26}H_{17}NS_3$ [M^+]: 439.0523; found: 439.0511.

Synthesis of 4

A flame-dried Schlenk tube was charged with **2b** (500 mg, 1.7 mmol, 1.5 equiv) and dry THF (approximately 20 mL). The solution was cooled to −78 °C before a solution of *n*BuLi in hexane

(1.6 м, 1.70 mL, 1.6 equiv) was added dropwise by means of a syringe. The solution turned brown and after 45 min at that temperature neat tributylborate (0.455 mL, 1.7 mmol, 1.5 equiv) was added. The low-temperature bath was removed and the solution was allowed to warm to RT over a period of 1 h or more. In the meantime, the solution turned red and then pale orange. Finally, the content was transferred by means of a syringe to a second Schlenk tube containing 4-bromothiazole (270 mg, 1.1 mmol, 1 equiv), sodium carbonate (179 mg, 1.7 mmol, 1.5 equiv), and tetrakis(triphenylphosphine) palladium(0) (39 mg, 3 mol %) dissolved in a degassed 1:1 mixture of DME/water. The combined solution was warmed at 65–75 °C until TLC showed reaction completion. The crude mixture was allowed to cool to RT, diluted with water, and extracted with ethyl acetate. The organic phase was combined, dried over anhydrous magnesium sulfate, filtered, and the solvent was removed. Purification by flash chromatography (silica, hexane/$CHCl_3$, 9/1, v/v) afforded **4** as a white powder (460 mg, 90 %). M.p. 145–148 °C; ^1H NMR (300 MHz, $CDCl_3$): $\delta = 3.87$ (s, 3 H), 6.80 (s, 1 H), 7.14–7.44 (m, 9 H), 7.76–7.98 ppm (m, 4 H); ^{13}C NMR (75 MHz, $CDCl_3$): $\delta = 61.7$, 109.2, 114.6, 122.0, 122.2, 122.3, 123.2, 123.3, 124.2, 124.3, 124.8, 125.0, 126.6, 128.9, 130.1, 131.3, 133.2, 136.6, 137.5, 138.9, 140.7, 149.5, 161.6, 166.6 ppm; IR: $\tilde{\nu} = 3133$, 3057, 3010, 1598, 1573, 1551, 1532, 1502, 1486, 1464, 1447, 1434, 1420, 1357, 1316, 1282, 1262, 1233, 1183, 1155, 1016, 1002, 763, 743, 724 cm^{-1}; HRMS (EI): m/z calcd for $C_{26}H_{18}NOS_3$ $[M+H]^+$: 456.0551; found: 456.0552.

Synthesis of 5

A Schlenk tube was charged with **2a** (250 mg, 0.9 mmol, 1 equiv), **D** (227 mg, 0.9 mmol, 1 equiv), PivOH (27 mg, 30 mol %), $P(tBu)_2MeHBF_4$ (22 mg, 10 mol %), anhydrous cesium carbonate (582 mg, 1.8 mmol, 2 equiv), and palladium(II) acetate (10 mg, 5 mol %) under a stream of nitrogen. Dry mesitylene was added by means of a syringe (3 mL) and the suspension was evacuated/backfilled with nitrogen several times. The mixture was heated at 140 °C (at high temperature the reactants solubilize and the reaction starts). The mixture was allowed to cool to RT and after TLC monitoring showed completion it was partitioned between an aqueous layer and ethyl acetate. The biphasic system was filtered through a pad of Celite and the organic phase was separated, dried over anhydrous magnesium sulfate, and filtered. After removal of the solvent, the crude product was purified by flash chromatography (silica, hexane/$CHCl_3$) to afford **5** as a white solid (250 mg, 62 %). M.p. 145–148 °C; ^1H NMR (300 MHz, $CDCl_3$): $\delta = 1.82$ (s, 3 H), 2.22 (s, 3 H), 7.18–7.43 (m, 11 H), 7.77–7.96 ppm (m, 4 H); ^{13}C NMR (75 MHz, $CDCl_3$): $\delta = 12.3$, 14.9, 121.9, 122.2, 123.0, 123.7, 123.9, 124.1, 124.2, 124.8, 126.3, 127.3, 128.7, 128.8, 129.7, 131.9, 133.5, 136.0, 138.2, 138.8, 139.5, 139.7, 139.8, 145.6, 164.1 ppm; IR: $\tilde{\nu} = 3054$, 2946, 1948, 1512, 1496, 1453, 1430, 1308, 1289, 1263, 1250, 1171, 1155, 1142, 1021, 971, 759, 740, 726 cm^{-1}; HRMS (EI): m/z calcd for $C_{26}H_{19}NS_3$ $[M^+]$: 453.0680; found: 453.0681.

Synthesis of 6

A Schlenk tube was charged with **2b** (200 mg, 0.7 mmol, 1 equiv), **D** (172 mg, 0.7 mmol, 1 equiv), PivOH (21 mg, 30 mol %), $P(tBu)_2MeHBF_4$ (17 mg, 10 mol %), anhydrous cesium carbonate (441 mg, 14 mmol, 2 equiv), and palladium(II) acetate (8 mg, 5 mol %) under a stream of nitrogen. Dry mesitylene was added by means of a syringe (2.3 mL) and the suspension was evacuated/backfilled with nitrogen several times. The mixture was heated at 140 °C (at high temperature the reactants solubilize and the reaction starts). The mixture was allowed to cool down RT and after TLC monitoring showed completion it was partitioned between an aqueous layer and ethyl acetate. The biphasic system was filtered through a pad of Celite and the organic phase was separated, dried over anhydrous magnesium sulfate, and filtered. After removal of the solvents, the crude product was purified by flash chromatography (silica, hexane/$CHCl_3$) to afford **6** as a white solid (270 mg, 85 %). M.p. 57–60 °C; ^1H NMR (300 MHz, $CDCl_3$): $\delta = 1.92$ (s, 3 H), 3.77 (s, 3 H), 7.14–7.42 (m, 8 H), 7.53 (d, 1 H, J = 6 Hz), 7.56 (d, 1 H, J = 6 Hz), 7.85–7.93 ppm (m, 3 H); ^{13}C NMR (75 MHz, $CDCl_3$): $\delta = 12.3$, 61.4, 109.8, 122.0, 122.2, 122.7, 123.9, 124.1, 124.7, 124.8, 126.3, 127.1, 128.8, 128.9, 129.7, 130.9, 131.7, 133.6, 135.5, 137.6, 139.2, 139.8, 146.0, 161.1, 163.9 ppm; IR: $\tilde{\nu} = 3058$, 2835, 1597, 1575, 1542, 1512, 1493, 1460, 1449, 1423, 1312, 1266, 1155, 1139, 1017, 756, 726 cm^{-1}; HRMS (EI): m/z calcd for $C_{27}H_{19}NOS_3$ $[M^+]$: 469.0629; found: 469.0619.

Synthesis of 7

A Schlenk tube was charged with benzothiophene (791 mg, 6 mmol, 3 equiv), **D** (500 mg, 2 mmol, 1 equiv), PivOH (60 mg, 30 mol %), $P(tBu)_2MeHBF_4$ (49 mg, 10 mol %), anhydrous cesium carbonate (1.28 g, 4 mmol, 2 equiv), and palladium(II) acetate (22 mg, 5 mol %) under a stream of nitrogen. Dry mesitylene was added by means of a syringe (3 mL) and the suspension was evacuated/backfilled with nitrogen several times. The mixture was heated at 140 °C (at high temperature the reactants solubilize and the reaction starts). The mixture was allowed to cool to RT and after TLC monitoring showed completion it was partitioned between an aqueous layer and ethyl acetate. The biphasic system was filtered through a pad of Celite and the organic phase was separated, dried over anhydrous magnesium sulfate, and filtered. After removal of solvent, the crude product was purified by column chromatography (silica, hexane/$CHCl_3$, 1:4, v/v) to afford **7** as a white solid (550 mg, 91 %). M.p. 95–97 °C; ^1H NMR (300 MHz, $CDCl_3$): $\delta = 2.70$ (s, 3 H), 7.31–7.58 (m, 5 H), 7.77 (s, 1 H), 7.79–7.97 ppm (m, 4 H); ^{13}C NMR (75 MHz, $CDCl_3$): $\delta = 13.0$, 121.4, 122.1, 123.6, 124.3, 126.3, 128.8, 129.0, 129.9, 133.3, 138.6, 139.7, 140.3, 145.8, 163.6 ppm; IR: $\tilde{\nu} = 3048$, 3018, 2852, 1493, 1455, 1440, 1311, 1244, 1197, 1152, 1125, 1067, 1015, 976, 826, 762, 744, 725 cm^{-1}; HRMS (EI): m/z calcd for $C_{18}H_{13}NS_2$ $[M^+]$: 307.0489; found: 307.0497.

Synthesis of 8

A brown-glass, round-bottomed flask was charged with **5** (400 mg, 1.3 mmol, 1 equiv) and THF (13 mL). NBS (255 mg, 1.4 mmol, 1.1 equiv) was added in one portion at 0 °C and the mixture was allowed to slowly warm to RT overnight. Water was added and the suspension was extracted with ethyl acetate. The organic phase was washed with an approximately 1 м aqueous solution of NaOH, then with water, dried over anhydrous magnesium sulfate, and finally filtered. The solvent was removed and the crude product was used without further purification (500 mg, 99 %). M.p. 88–90 °C; ^1H NMR (300 MHz, $CDCl_3$): $\delta = 2.51$ (s, 3 H), 7.38–7.46 (m, 5 H), 7.79–7.95 (m, 4 H); ^{13}C NMR (75 MHz, $CDCl_3$): $\delta = 13.2$, 108.4, 122.2, 123.6, 125.1, 125.7, 126.3, 128.8, 129.9, 132.4, 133.3, 133.6, 138.1, 138.6, 144.1, 164.7 ppm; IR: $\tilde{\nu} = 3058$, 2920, 2847, 1505, 1489, 1488, 1460, 1437, 1306, 1277, 1250, 1162, 1070, 1017, 968, 814, 749, 719 ppm; HRMS (EI): m/z calcd for $C_{18}H_1NBrS_2$ $[M^+]$: 384.9595; found 384.9606.

Synthesis of 9

A Schlenk tube equipped with a magnetic stirring bar and capped with a rubber septum was charged with **6** (361 mg, 0.9 mmol, 1 equiv), commercially available benzo[*b*]thiophen-3-yl boronic acid (250 mg, 1.4 mmol, 1.5 equiv), and anhydrous potassium carbonate (194 mg, 1.4 mmol, 1.5 equiv). DME (23 mL) was then added and the suspension was evacuated/backfilled with nitrogen several times. Tetrakis(triphenylphosphine) palladium(0) (32 mg, 3 mol %) was added under a stream of nitrogen, followed by distilled water (12 mL), and the monophasic mixture was evacuated/backfilled again. The solution was heated at 60–75 °C over a period of 24 h (TLC monitoring) and allowed to cool to RT. After diluting the mixture with water, the aqueous layer (purple) was extracted with ethyl acetate several times. The organic phases were combined, dried over anhydrous magnesium sulfate, filtered, and the solvent was removed. The crude product was purified by flash column chromatography (silica, hexane/$CHCl_3$) to afford **9** as a white solid (340 mg, 83 %). M.p. 70 °C; ^1H NMR (300 MHz, $CDCl_3$): $\delta = 2.44$ (s, 3 H), 7.22–7.44 (m, 6 H), 7.54 (s, 1 H), 7.81 (d, 1 H, $J = 6$ Hz), 7.95 ppm (d, 1 H, $J = 6$ Hz); ^{13}C NMR (75 MHz, $CDCl_3$): $\delta = 14.8$, 122.0, 122.6, 122.8, 123.2, 123.4, 123.9, 124.1, 124.2, 124.3, 124.5, 124.6, 124.7, 125.6, 127.5, 130.7, 138.2, 138.3, 138.8, 140.0, 140.4 ppm; IR: $\tilde{\nu} = 3058$, 2913, 1575, 1456, 1437, 1420, 1312, 1286, 1250, 1237, 1155, 1070, 1021, 972, 756, 726 cm^{-1}; HRMS (EI): *m/z* calcd for $C_{26}H_{17}NS_3$ [M^+]: 439.0523; found: 439.0520.

Acknowledgements

We thank the Japan Society for Promotion of Science (JSPS) and the Centre National de la Recherche Scientifique (CNRS) for their financial support. A part of the present study has been supported with a Grant-in-Aid for Scientific Research on Priority-Area, Photosynergetics.

Keywords: arylation · helical structures · isomerization · photochromism · substituent effects

[1] a) *Photochromism*, Wiley-Interscience, New-York, **1971**; b) H. Dürr, H. Bouas-Laurent in *Photochromism, Molecules and Systems, Studies in Organic Chemistry 40*, Elsevier, Amsterdam, **1990**.

[2] a) V. Balzani, A. Credi, M. Venturi in *Molecular Devices and Machines: A Journey into the Nano World*, Wiley-VCH, Weinheim, **2003**; b) J. A. Delaire, K. Nakatani, *Chem. Rev.* **2000**, *100*, 1817 – 1816; c) Y. Hasegawa, T. Nakagawa, T. Kawai, *Coord. Chem. Rev.* **2010**, *254*, 2643 – 2651; d) M. Irie, *Chem. Rev.* **2000**, *100*, 1684 – 1716; e) Y. Yokoyama, *Chem. Rev.* **2000**, *100*, 1717 – 1740.

[3] a) M. Irie, T. Fukaminato, T. Sasaki, N. Tamai, T. Kawai, *Nature* **2002**, *420*, 759; b) V. Guerchais, L. Ordonneau, H. Le Bozec, *Coord. Chem. Rev.* **2010**, *254*, 2533 – 2545; c) H. Tian, S. Yang, *Chem. Soc. Rev.* **2004**, *33*, 85 – 97; d) G. Szalóki, G. Sevez, J. Berthet, J. L. Pozzo, S. Delbaere, *J. Am. Chem. Soc.* **2014**, *136*, 13510 – 13513; e) S. Takami, T. Kawai, M. Irie, *Eur. J. Org. Chem.* **2002**, 3796 – 3800; f) H. Nishi, T. Namari, S. Kobatake, *J. Mater. Chem.* **2011**, *21*, 17249 – 17258; g) H. Shoji, D. Kitagawa, S. Kobatake, *Chem. Commun.* **2014**, *38*, 933 – 941; h) Y. C. Jeong, S. I. Yang, K. H. Ahn, E. Kim, *Chenm. Comm.* **2005**, 2503 – 2505; i) K. Uno, H. Niikura, M. Morimoto, Y. Ishibashi, H. Miyasaka, M. Irie, *J. Am. Chem. Soc.* **2011**, *133*, 13558 – 13564; j) H. Nitadori, L. Ordonneau, J. Boixel, D. Jacquemin, A. Boucekkine, A. Singh, M. Akita, I. Ledoux, V. Guerchais, H. Le Bozec, *Chem. Commun.* **2012**, *48*, 10395 – 10397; k) F. Meng, Y.-M. Hervault, Q. Shao, B. Hu, L. Norel, S. Rigaut, X. Chen, *Nat. Commun.* **2013**, *5*, 3023 – 3032; l) M. Irie, T. Fukaminato, K. Matsuda, S. Kobatake, *Chem. Rev.* **2014**, *114*, 12174 – 12277.

[4] a) G. Szalóki, J. L. Pozzo, *Chem. Eur. J.* **2013**, *19*, 11124 – 11132; b) K. Beydoun, J. Roger, J. Boixel, H. Le Bozec, V. Guerchais, H. Doucet, *Chem. Commun.* **2012**, *48*, 11951 – 11953.

[5] a) L. N. Lucas, J. J. D. de Jong, J. H. van Esch, R. M. Kellogg, B. L. Feringa, *Eur. J. Org. Chem.* **2003**, 155 – 166; b) R. Göstl, S. Hecht, *Angew. Chem. Int. Ed.* **2014**, *53*, 8784 – 8787.

[6] R. Göstl, B. Kobin, L. Grubert, M. Pätzel, S. Hecht, *Chem. Eur. J.* **2012**, *18*, 14282 – 14285.

[7] For recent examples, see: a) T. Nakashima, K. Atsumi, S. Kawai, T. Nakagawa, Y. Hasegawa, T. Kawai, *Eur. J. Org. Chem.* **2009**, 3112 – 3218; b) H. L. Wong, W.-T. Wong, V. W.-W. Yam, *Org. Lett.* **2012**, *14*, 1862 – 1865; c) C. T. Poon, V. W.-W. Lam, *J. Am. Chem. Soc.* **2011**, *133*, 19622 – 19625; d) J. C.-H. Chan, W.-H. Lam, H. L. Wong, W. T. Wong, V. W.-W. Yam, *Angew. Chem. Int. Ed.* **2013**, *52*, 11504 – 11508; *Angew. Chem.* **2013**, *125*, 11718 – 11722.

[8] S. Fukumoto, T. Nakashima, T. Kawai, *Dyes Pigm.* **2012**, *92*, 868 – 871.

[9] a) K. Morinaka, T. Ubukata, Y. Yokoyama, *Org. Lett.* **2009**, *11*, 3890 – 3893; b) M. Kose, E. Orhan, K. Suzuki, A. Tutar, C. Uenlue, Y. Yokoyama, *J. Photochem. Photobiol. A* **2013**, *257*, 50 – 53; c) H. Ogawa, K. Takagi, T, Ubakata, A. Okamoto, N. Yonezawa, S. Delbaere, Y. Tokoyama, *Chem. Commun.* **2012**, *48*, 11838 – 11840; d) F. G. Erko, J. Berthet, H. Ogawa, Y. Yokoyama, S. Delbaere, *Tetrahedron Lett.* **2013**, *54*, 6366 – 6369.

[10] a) B. M. Neilson, V. M. Lynch, C. W. Bielawski, *Angew. Chem. Int. Ed.* **2011**, *50*, 10322 – 10326; *Angew. Chem.* **2011**, *123*, 10506 – 10510; b) B. M. Neilson, C. W. Bielawski, *J. Am. Chem. Soc.* **2012**, *134*, 12693 – 12699; c) V. W.-W. Yam, J. K.-W. Lee, C.-C. Ko, N. Zhu, *J. Am. Chem. Soc.* **2009**, *131*, 912 – 913; d) P. H.-M. Lee, C.-C. Ko, N. Zhu, V. W.-W. Yam, *J. Am. Chem. Soc.* **2007**, *129*, 6058 – 6059; e) T. Nakashima, M. Goto, S. Kawai, T. Kawai, *J. Am. Chem. Soc.* **2008**, *130*, 14570 – 14575.

[11] a) T. Nakashima, K. Atsumi, S. Kawai, T. Nakagawa, Y. Hasegawa, T. Kawai, *Eur. J. Org. Chem.* **2007**, 3212 – 3218; b) K. Ouhenia-Ouadahi, R. Yasukuni, P. Yu, G. Laurent, C. Pavageau, J. Grand, J. Guérin, A. Léaustic, N. Félidj, J. Aubard, K. Nakatani, R. Métivier, *Chem. Commun.* **2014**, *50*, 7299 – 7302; c) T. Nakagawa, K. Atsumi, T. Nakashima, Y. Hasegawa, T. Kawai, *Chem. Lett.* **2007**, *36*, 372 – 373; d) T. Nakagawa, Y. Hasegawa, T. Kawai, *J. Phys. Chem. A* **2008**, *112*, 5096 – 5103; e) Y. Kutsunugi, S. Kawai, T. Nakashima, T. Kawai, *New. J. Chem.* **2009**, *33*, 1368 – 1373; f) H. Nakagawa, S. Kawai, T. Nakashima, T. Kawai, *Org. Lett.* **2009**, *11*, 1475 – 1478; g) M. Taguchi, T. Nakagawa, T. Nakashima, T. Kawai, *J. Mater. Chem.* **2011**, *21*, 17425 – 17432; h) M. Taguchi, T. Nakagawa, T. Nakashima, C. Adachi, T. Kawai, *Chem. Commun.* **2013**, *49*, 6373 – 6375.

[12] a) W. Zhu, Y. Yang, R. Métivier, Q. Zhang, R. Guillot, Y. Xie, H. Tian, K. Nakatani, *Angew. Chem. Int. Ed.* **2011**, *50*, 10986 – 10990; *Angew. Chem.* **2011**, *123*, 11178 – 11182; b) W. Li, C. Jiao, X. Li, Y. Xie, K. Nakatani, H. Tian, W. Zhu, *Angew. Chem. Int. Ed.* **2014**, *53*, 4603 – 4607.

[13] a) S. Chen, Y. Yang, Y. Wu, H. Tian, W. Zhu, *J. Mater. Chem.* **2012**, *22*, 5486 – 5494; b) Y.-C. Jeong, C. Gao, I. S. Lee, S. I. Yang, K.-H. Ahn, *Tetrahedron Lett.* **2009**, *50*, 5288 – 5290; c) S. Cheng, L.-J. Chen, H.-B. Yang, H. Tian, W. Zhu, *J. Am. Chem. Soc.* **2012**, *134*, 13596 – 13599; d) S. Fukumoto, T. Nakashima, T. Kawai, *Angew. Chem. Int. Ed.* **2011**, *50*, 1565 – 1568; *Angew. Chem.* **2011**, *123*, 1603 – 1606.

[14] K. Yuan, J. Boixel, A. Chantzis, D. Jacquemin, V. Guerchais, H. Doucet, *Chem. Eur. J.* **2014**, *20*, 10073 – 10083.

[15] a) R. Sanz, V. Guilarte, E. Hernando, A. M. Sanjuán, *J. Org. Chem.* **2010**, *75*, 7443 – 7446; b) A. Heynderickx, A. Samat, R. Guglielmetti, *Synthesis* **2002**, 213 – 216.

[16] B. Liégault, I. Petrov, S. I. Gorelsky, K. Fagnou, *J. Org. Chem.* **2010**, *75*, 1047 – 1060.

[17] A. G. Lvov, V. Z. Shirinian, V. V. Kachala, A. M. Kavun, I. V. Zavarin, M. M. Krayushkin, *Org. Lett.* **2014**, *16*, 4532 – 4535.

[18] a) S. Nakamura, T. Kobayashi, A. Takata, K. Uchida, Y. Asano, A. Murakami, A. Goldberg, D. Guillaumont, S. Yokojima, S. Kobatake, M. Irie, *J. Phys. Org. Chem.* **2007**, *20*, 821 – 829; b) K. Morimitsu, K. Shibata, S. Kobatake, M. Irie, *J. Org. Chem.* **2002**, *67*, 4574 – 4578; c) T. Fukaminato, T. Umemoto, Y. Iwata, S. Yokojima, M. Yoneyama, S. Nakamura, M. Irie, *J. Am. Chem. Soc.* **2007**, *129*, 5932 – 5938; d) S. Kobatake, Y. Matsumoto, M. Irie, *Angew. Chem. Int. Ed.* **2005**, *44*, 2148 – 2151; *Angew. Chem.* **2005**, *117*, 2186 – 2189; e) A. de Meijere, Z. Ligang, V. N. Belov, M. Bossi, N. Noltmeyer, W. S. Hell, *Chem. Eur. J.* **2007**, *13*, 2503 – 2516; f) T. Fukaminato, T. Sasaki, T. Kawai, N. Tamai, M. Irie, *J. Am. Chem. Soc.* **2004**, *126*, 14843 – 14849.

[19] J. Massaad, J.-C. Micheau, C. Coudret, R. Sanchez, G. Guirado, S. Delbaere, *Chem. Eur. J.* **2012**, *18*, 6568 – 6575. See also a) S. Delbaere, J. Berthet, T. Shiozawa, Y. Yokoyama, *J. Org. Chem.* **2012**, *77*, 1853 – 1859;

b) ref. [6]; c) S. Aloïse, M. Sliwa, G. Buntinx, S. Delbaere, A. Perrier, F. Maurel, D. Jacquemin, M. Takeshita, *Phys. Chem. Chem. Phys.* **2013**, *15*, 6226–6234; d) O. Galangau, Y. Kimura, R. Kanazawa, T. Nakashima, T. Kawai, *Eur. J. Org. Chem.* **2014**, 7165–7173.

[20] a) Naraso, F. Wudl, *Macromolecules* **2008**, *41*, 3169–3174; b) M. Karikomi, C. Kitamura, S. Tanaka, Y. Yamashita, *J. Am. Chem. Soc.* **1995**, *117*, 6791–6792.

[21] E. R. Johnson, S. Keinan, P. Mori-Sanchez, J. Contreras-García, A. J. Cohen, W. Yang, *J. Am. Chem. Soc.* **2010**, *132*, 6498–6506.

[22] For general reviews on helicenes, see: a) Y. Shen, C.-F. Chen, *Chem. Rev.* **2012**, *112*, 1463–1535; b) T. Okuyama, Y. Tani, K. Miyake, Y. Yokoyama, *J. Org. Chem.* **2007**, *72*, 1634–1638. See also: c) L. Norel, M. Rudolph, N. Vanthuyne, J. A. G. Williams, C. Lescop, C. Roussel, J. Autschbach, J. Crassous, R. Réau, *Angew. Chem. Int. Ed.* **2010**, *49*, 99–102; *Angew. Chem.* **2010**, *122*, 103–106; d) J.-D. Chen, H.-Y. Lu, C.-F. Chen, *Chem. Eur. J.* **2010**, *16*, 11843–11846; e) T. B. Norsten, A. Peters, R. McDonald, M. Wang, N. R. Branda, *J. Am. Chem. Soc.* **2001**, *123*, 7447–7448; f) T. J. Wigglesworth, D. Sud, T. B. Norsten, V. S. Lekhi, N. R. Branda, *J. Am. Chem. Soc.* **2005**, *127*, 7272–7273.

[23] N. Ito, T. Hirose, K. Matsuda, *Org. Lett.* **2014**, *16*, 2502–2505.

Received: February 15, 2015

FULL PAPER

Simple substitutions: The preparation of five new benzothiophene-centered terarylene pro-helical derivatives is described. They display various and opposite photoactivities, depending on substitution at the reactive centers (see figure). When fully substituted, ring cyclization generates stable [5]helical derivatives with outstanding absorption properties.

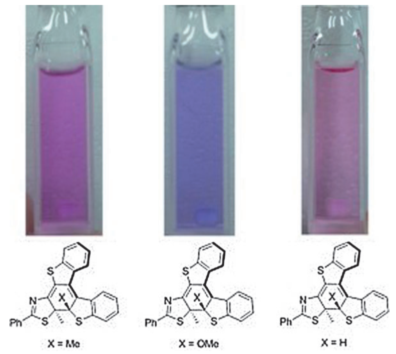

Helical Structures

O. Galangau, T. Nakashima, F. Maurel, T. Kawai**

■■ – ■■

Substituent Effects on the Photochromic Properties of Benzothiophene-Based Derivatives